

# Topical Losartan and Corticosteroid Additively Inhibit Corneal Stromal Myofibroblast Generation and Scarring Fibrosis After Alkali Burn Injury

Lycia Pedral Sampaio<sup>1,2</sup>, Guilherme S. L. Hilgert<sup>1</sup>, Thomas Michael Shiju<sup>1</sup>, Marcony R. Santhiago<sup>2</sup>, and Steven E. Wilson<sup>1</sup>

<sup>1</sup> Cole Eye Institute, Cleveland Clinic, Cleveland, OH, USA

<sup>2</sup> Department of Ophthalmology at University of São Paulo, São Paulo, Brazil

**Correspondence:** Steven E. Wilson, Cole Eye Institute, I-32, Cleveland Clinic, 9500 Euclid Ave, Cleveland, OH, USA.

e-mail: [wilsons4@ccf.org](mailto:wilsons4@ccf.org)

**Received:** May 19, 2022

**Accepted:** June 19, 2022

**Published:** July 12, 2022

**Keywords:** cornea; fibrosis; scarring; alkali burn; losartan; corticosteroids; myofibroblasts; keratocan; corneal fibroblasts; corneal endothelium; basement membranes; collagen type IV; TGF  $\beta$ -1

**Citation:** Sampaio LP, Hilgert GSL, Shiju TM, Santhiago MR, Wilson SE. Topical losartan and corticosteroid additively inhibit corneal stromal myofibroblast generation and scarring fibrosis after alkali burn injury. *Transl Vis Sci Technol*. 2022;11(7):9, <https://doi.org/10.1167/tvst.11.7.9>

**Purpose:** To evaluate the efficacy of losartan and prednisolone acetate in inhibiting corneal scarring fibrosis after alkali burn injury in rabbits.

**Methods:** Sixteen New Zealand White rabbits were included. Alkali injuries were produced using 1N sodium hydroxide on a 5-mm diameter Whatman #1 filter paper for 1 minute. Four corneas in each group were treated six times per day for 1 month with 50  $\mu$ L of (1) 0.2 mg/mL losartan in balanced salt solution (BSS), (2) 1% prednisolone acetate, (3) combined 0.2 mg/mL losartan and 1% prednisolone acetate, or (4) BSS. Area of opacity and total opacity were analyzed in standardized slit-lamp photos with ImageJ. Corneas in both groups were cryofixed in Optimal cutting temperature (OCT) compound at 1 month after surgery, and immunohistochemistry was performed for alpha-smooth muscle actin ( $\alpha$ -SMA) and keratocan or transforming growth factor  $\beta$ 1 and collagen type IV with ImageJ quantitation.

**Results:** Combined topical losartan and prednisolone acetate significantly decreased slit-lamp opacity area and intensity, as well as decreased stromal myofibroblast  $\alpha$ -SMA area and intensity of staining per section and confined myofibroblasts to only the posterior stroma with repopulation of the anterior and mid-stroma with keratocan-positive keratocytes after 1 month of treatment. Corneal fibroblasts produced collagen type IV not associated with basement membranes, and this production was decreased by topical losartan.

**Conclusions:** Combined topical losartan and prednisolone acetate decreased myofibroblast-associated fibrosis after corneal alkali burns that produced full-thickness injury, including corneal endothelial damage. Increased dosages and duration of treatment may further decrease scarring fibrosis.

**Translational Relevance:** Topical losartan and prednisolone acetate decrease myofibroblast-mediated scarring fibrosis after corneal injury.

## Introduction

Corneal scarring caused by the development of myofibroblasts and fibrosis after microbial infections, traumatic injury, scarring diseases, and complications after corneal surgeries is one of the most important causes of vision loss in the United States and throughout the world.<sup>1</sup> World Health Organization studies

noted that 5.1% of bilateral blindness is corneal in etiology, and stromal scarring was the largest subcategory in that group.<sup>1</sup>

The complex corneal wound-healing response to injury has been detailed in previous reviews.<sup>2,3</sup> Although numerous growth factors and cytokines, such as platelet-derived growth factor (PDGF) and interleukin 1 $\alpha$ , serve to modulate these processes, depending on the location, extent of injury, and other

factors, many studies have demonstrated that the transforming growth factor (TGF)  $\beta$  isotypes are the most important growth factors modulating the development and persistence of myofibroblasts and are key to generating or eliminating stromal scarring fibrosis.<sup>4–6</sup> Losartan is an angiotensin-converting enzyme II receptor antagonist that has been shown in numerous studies to inhibit TGF- $\beta$  signaling.<sup>7–13</sup> The specific mechanism(s) through which losartan inhibits TGF- $\beta$  signaling have not been fully characterized. One study found that losartan interfered with the SMAD signaling pathways.<sup>14</sup> Another study found that losartan inhibited the expression of SMAD2.<sup>15</sup> Yet another study found that losartan inhibited noncanonical TGF- $\beta$  signaling by indirect inhibition of ERK activation.<sup>16</sup> Thus, there may be several SMAD-related mechanisms through which losartan has its inhibitory effect on TGF- $\beta$  signaling. Most studies, however, showed that losartan inhibited the end effect of known TGF- $\beta$ -mediated processes in injury models in other tissues and did not investigate the specific mechanisms.

Recent studies have demonstrated that the epithelial basement membrane (BM)<sup>5,17–20</sup> and Descemet's BM<sup>19,21,22</sup> are also critical modulators of corneal scarring fibrosis through BM component modulation of TGF- $\beta$  entry into the corneal stroma from the epithelium, tears, aqueous humor, and residual corneal endothelium. Another study demonstrated that topical, but not oral, losartan decreased TGF- $\beta$ -mediated myofibroblast development and stromal fibrosis after removal of the central Descemet's membrane and corneal endothelial complex (descemetorhexis) in rabbits.<sup>7</sup>

The purpose of the current study was to test the hypothesis that topical losartan and/or prednisolone acetate would inhibit stromal scarring, myofibroblast generation, and fibrosis in rabbit corneas after severe alkali burn injuries. The effect of these treatments on stromal collagen type IV production was also investigated.

## Materials and Methods

### Animals

All animal treatments and care were approved by the Institutional Animal Care and Use Committee at the Cleveland Clinic Foundation (Cleveland, OH, USA) and the Animal Care and Use Review Office of the Department of the Army (Fort Detrick, MD, USA). All rabbits were treated in accordance with the tenets of the ARVO Statement for the Use of Animals in Ophthalmic and Vision Research. Sixteen 10- to

15-week-old female New Zealand White rabbits weighing 2.5 to 3.0 kg each were included in this study.

### Corneal Alkali Burn Method

Beginning 24 hours prior to alkali exposure and continuing for 5 to 7 days after treatment, rabbits received 60 mL children's liquid acetaminophen (Johnson & Johnson, Ft. Washington, PA, USA) per 1 L of drinking water. Prior to all alkali exposures and testing, the rabbits were anesthetized with 30 mg/kg ketamine hydrochloride and xylazine 5 mg/kg by intramuscular injection. In addition, topical proparacaine hydrochloride 1% (Alcon, Ft Worth, TX, USA) was applied to each eye. As needed, due to signs of pain, rabbits also received 0.05 mg/kg buprenorphine by subcutaneous injection twice a day.

Alkali injuries were produced in one eye of rabbits with previously published methods<sup>23</sup> using 1N sodium hydroxide (Sigma, St. Louis, MO, USA) in balanced salt solution (BSS; 0.64% sodium chloride, 0.075% potassium chloride, 0.048% calcium chloride dihydrate, 0.03% magnesium chloride hexahydrate, 0.39% sodium acetate trihydrate, 0.17% sodium citrate dihydrate, pH 7.5; Alcon) and a 5-mm diameter circular Whatman No. 1 filter paper (cat. 1001-6508; Fisher Scientific, Pittsburgh, PA) wetted with 100  $\mu$ L 1N sodium hydroxide (NaOH) solution. Following the alkali burn injury, the cornea was irrigated profusely with BSS. Each injured cornea also received one drop of ciprofloxacin (Alcon) 10 minutes after surgery and four times a day for 1 week and at least 15 minutes apart from the study medications.

### Treatment With Topical Losartan and/or Prednisolone Acetate

Beginning immediately following alkali burn injury, four corneas in each group were treated six times per day (approximately 8 AM, 10 AM, 12 noon, 2 PM, 4 PM, and 6 PM) for 1 month with (1) 50  $\mu$ L 0.2 mg/mL losartan (Merck & Co., Inc., Kenilworth, NJ, USA) in BSS, (2) 50  $\mu$ L 1% prednisolone acetate (Alcon), (3) 50  $\mu$ L 0.2 mg/mL losartan in BSS and 50  $\mu$ L 1% prednisolone acetate (Alcon) at least 5 minutes apart, or (4) 50  $\mu$ L BSS.

### Fluorescein Staining for Epithelial Defects at 2 Weeks After Injury

At 2 weeks after alkali burn injury, topical 0.5% fluorescein in BSS was applied to each eye, and

**Table 1.** Primary and Secondary Antibodies

Antigen	Company	Species	Ab Isotype	Catalog	Dilution
<b>Primary</b>					
Keratocan	Winston Kao	Goat	IgG	—	1:200
SMA	Dako	Mouse	IgG <sub>2a</sub>	M0851	1:400
TGF- $\beta$ 1	Genetex	Mouse	IgG <sub>1</sub>	GTX21279	1:100
Collagen type IV	Millipore	Goat	IgG1	AB769	1:2000
<b>Secondary</b>					
Alexa Fluor 488 anti-mouse	TFS <sup>a</sup>	Donkey	IgG	A21202	1:200
Alexa Fluor 488 anti-goat	TFS	Donkey	IgG	A11055	1:200
Alexa Fluor 568 anti-mouse	TFS	Donkey	IgG	A10037	1:200
Alexa Fluor 568 anti-goat	TFS	Donkey	IgG	A11057	1:200

<sup>a</sup>TFS is Thermo Fisher Scientific.

the presence or absence of epithelial defect(s) was recorded.

### Standardized Slit-Lamp Photographs, Corneal Angiography, and ImageJ Analysis of Corneal Opacity

At 1 month after sodium hydroxide exposure and treatments, with the rabbits under ketamine-xylazine general anesthesia, the eyes were dilated with two drops of 1% tropicamide (Akorn Co., Lake Forest, IL, USA) for 30 minutes. The study eye in each rabbit had slit-lamp photographs with standardized illumination level and angle of illumination at 20 $\times$  magnification with a Topcon (Oakland, NJ, USA) SL-D7 slit-lamp photography system. For each study eye, the total area of opacity was determined by outlining the opacity with the freehand selection tool using ImageJ 1.53a analysis software (National Institutes of Health, Bethesda, MD, USA) calibrated to mm<sup>2</sup>. The “raw internal density” in pixels for the opacified area in each cornea was also determined using ImageJ.

All corneas had fluorescent angiography at the peak of dye passage in the cornea immediately after injection of 1.5 mL 10% sodium fluorescein (McKesson, Irvine, TX, USA) in the central ear vein with the slit-lamp system and digital camera system using a “barrier filter” that only transmitted 520 to 530 nm, the peak of fluorescein emission, with broad illumination of the cornea, as previously described.<sup>24</sup>

### Corneal Fixation and Sectioning

One month after exposure and topical treatment, rabbits were euthanized after ketamine-xylazine general anesthesia with 100 mg/kg Beuthanasia (Shering-Plough, Kenilworth, NJ, USA) by intra-

venous injection and bilateral pneumothorax. The corneo-scleral rims of eyes were removed with sharp Westcott scissors (Fairfield, CT, USA) and 0.12 forceps (Storz, St Louis, MO, USA). The cornea was centered in a 24-mm  $\times$  24-mm  $\times$  5-mm mold (Fisher Scientific, Pittsburgh, PA, USA) that was filled with optimal cutting temperature (OCT) compound (Sakura Finetek, Torrance, CA, USA) and quick frozen on dry ice. Blocks were stored at  $-80^{\circ}\text{C}$  until sectioning.

OCT blocks were bisected at the center of the cornea and 8- $\mu\text{m}$ -thick transverse sections were cut from the central cornea with a cryostat (HM 505M; Micron GmbH, Walldorf, Germany). Three sections from each cornea were placed on each 25-mm  $\times$  75-mm  $\times$  1-mm Superfrost Plus microscope slide (Fisher Scientific). Slides with sections were maintained at  $-20^{\circ}\text{C}$  prior to immunohistochemistry (IHC).

### Immunohistochemistry and Fibrotic Area Opacity Intensity Analysis

Multiplex IHC was performed using previously described methods<sup>22</sup> and primary antibodies (Table 1) confirmed by Western blotting and IHC to recognize rabbit antigens or isotypic control antibodies (Thermo Fisher Scientific, Waltham, MA, USA) and secondary fluorescent tagged antibodies (Table 1). The collagen type IV antibody (cat. AB769; Millipore, Temecula, CA, USA) was raised against purified human and bovine collagen type IV that had been affinity purified with human and bovine collagen type IV crosslinked to agarose and cross-absorbed by the manufacturer with human and bovine collagens type I, II, III, V, and VI to eliminate cross-reactivity. This collagen type IV antibody was shown previously to bind rabbit collagen IV in IHC<sup>7,22</sup> and recognizes the  $\alpha$ -1/ $\alpha$ -2 chains but not the  $\alpha$ -3 to  $\alpha$ -6 chains. Winston Kao, PhD,

gifted the keratocan antibody raised against peptide H2N-LRLDGNEIKPPIPIDLVAC-OH. This marker was used to identify keratocytes in situ. The TGF- $\beta$ 1 antibody (GeneTex, Irvine, CA, USA) binds rabbit TGF- $\beta$ 1 in IHC and shows no reactivity to TGF- $\beta$ 2 or TGF- $\beta$ 3.<sup>5</sup>

The area of the  $\alpha$ -smooth muscle actin ( $\alpha$ -SMA)-positive stroma in mm<sup>2</sup> and the total  $\alpha$ -SMA opacity in pixels were quantitated using standardized images obtained with a 10 $\times$  objective on a Leica DM6B upright microscope equipped with an automated stage and Leica 7000 T camera using the LAS X software (Leica Microsystems, GmbH, Wetzlar, Germany). The means of three central corneal sections were analyzed from each cornea to provide the area of  $\alpha$ -SMA-positive stroma and the total  $\alpha$ -SMA opacity. The area of  $\alpha$ -SMA-positive stroma in mm<sup>2</sup> for each cornea was determined from full-diameter and full-thickness central corneal section images (all converted to 300 DPI, 885 width  $\times$  500 height, files with identical +50% brightness increase in Photoshop for all images) with the ImageJ 1.53a analysis software using the freehand selection tool to delineate the area(s) of  $\alpha$ -SMA-positive staining. In some corneas, two or more separated areas were present, and the summation of these areas was used as the value for that cornea. In these same sections for each cornea, the total  $\alpha$ -SMA-positive intensity in pixels was also determined with ImageJ, similarly by using the summation if separate  $\alpha$ -SMA-positive areas were present.

## Immunohistochemistry for Collagen Type IV and Quantitation

All corneas in each group had IHC for collagen type IV. Images from each cornea were converted to uniform 300 DPI, 875  $\times$  568 pixel files. Each cornea had three measurements of signal intensity in three randomly positioned 100  $\times$  50 ImageJ analysis rectangles in both the anterior cornea (anterior side of rectangle at the anterior stromal surface posterior to the epithelial basement membrane (EBM), if present) and posterior cornea (posterior side of rectangle at the posterior stromal surface anterior to Descemet's membrane, if present). The staining intensity within each box was determined with the analyze histogram function, and the mean of three boxes was the intensity value in the anterior or posterior stroma for that cornea.

## Statistics

Statistical analyses were performed using the Kruskal-Wallis test (<https://www.statskingdom.com/kruskal-wallis-calculator.html>), and  $P < 0.05$  was considered statistically significant.

## Results

### Persistent Epithelial Defects after Alkali Burn

At 2 and 4 weeks after the alkali burn, all corneas in all groups had at least a 1-mm diameter epithelial defect, and no differences between the treatment groups were found.

### Slit-Lamp Stromal Opacity and Central Corneal Neovascularization after Alkali Burn

Using the 100- $\mu$ L 1N NaOH on a 5-mm filter paper circle for a 1-minute method, followed by treatment with topical 0.2 mg/mL losartan, 1% prednisolone acetate, 0.2 mg/mL losartan, and 1% prednisolone acetate, or BSS vehicle, six times per day for 1 month, central stromal opacity of each of the corneas was as shown in Figure 1A. Examples of ImageJ delineations used to measure total stromal opacity area are shown in one cornea for each treatment. Notice that these quantitation areas contained a much denser center (\*in LOS-2, for example) and a less dense periphery (\*\*in LOS-2, for example) for each imaged cornea. The total area of opacity in mm<sup>2</sup> for each cornea in each group is shown in Figure 1B. Statistical comparisons between the groups are shown in Table 2. The losartan-alone, prednisolone-alone, and combined losartan and prednisolone groups were significantly different from the BSS vehicle group but not significantly different from each other. ImageJ was also used to determine the total opacity intensity in pixels for the combined dense central and less dense peripheral area in each cornea (as indicated by the dashed line in one cornea from each group) and that data are shown in Figure 1C. Statistical comparisons between the groups are shown in Table 3. The losartan-alone and combined losartan and prednisolone acetate groups were significantly different from the BSS vehicle group but not significantly different from each other. The difference between the 1% prednisolone acetate group and the BSS vehicle group did not reach statistical significance. The combined losartan and prednisolone acetate group, however, had the lowest standard error of the mean for both stromal opacity area and total opacity intensity.

Central corneal neovascularization (CNV; Supplementary Fig. S1) developed in all four BSS vehicle-treated corneas, in two corneas treated with topical 0.2 mg/mL losartan alone, in one of the corneas treated with 1% prednisolone acetate alone, and in none of the corneas treated with both 0.2 mg/mL losartan and 1% prednisolone acetate.



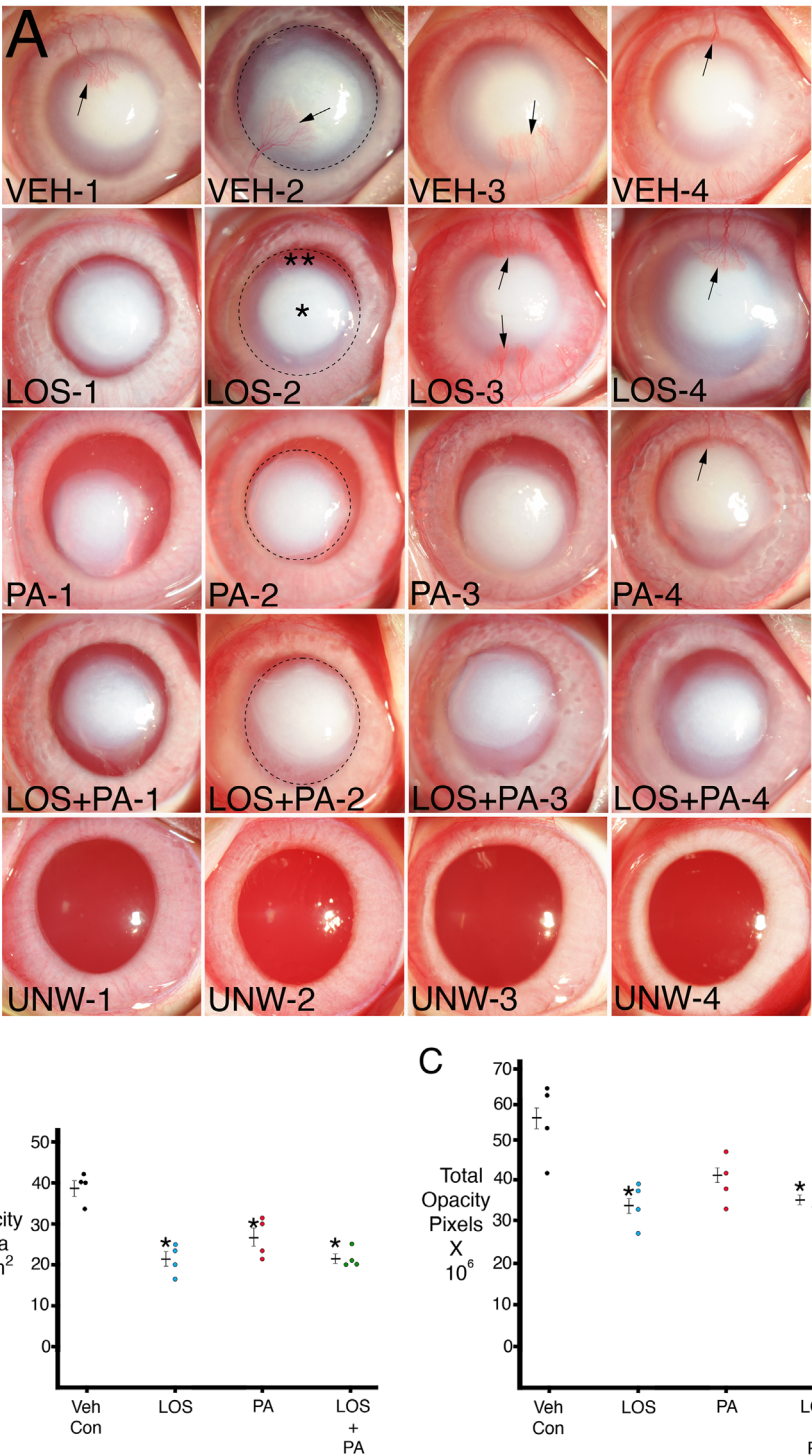


**Figure 1.** (A) Standardized slit-lamp photos of rabbit corneas at 1 month after a 1-minute exposure to 1N NaOH on a 5-mm diameter filter paper and continuous treatment for 1 month with topical vehicle (VEH), 0.2 mg/mL losartan, 1% prednisolone acetate, or 0.2 mg/mL losartan + 1% prednisolone acetate six times per day. Note that opacity in each cornea is made up of central more dense (\*) and peripheral less dense (\*\*) zones. Arrows indicate central corneal neovascularization. Dotted circles show examples of ImageJ analysis of total opacity for individual corneas that include the combined more dense central and less dense peripheral zones. UNW-1 to UNW-4 are unwounded and untreated controls for comparison. Magnification 15 $\times$ . (B) Graph of total opacity area measured with ImageJ in individual corneas. Mean  $\pm$  standard error of the mean is shown for each group. \* indicates the opacity was significantly different from the vehicle BSS control group. Table 2 shows Kruskal–Wallis *P* values for comparisons between the groups. (C) Graph of total opacity in pixels intensity measured with ImageJ in individual corneas. Mean  $\pm$  standard error of the mean is shown for each group. \* indicates the opacity was significantly different from the vehicle BSS control group. Table 3 shows Kruskal–Wallis *P* values for comparisons between the groups.

**Table 2.** Kruskal–Wallis *P* Values Slit-Lamp Opacity Area

Characteristic	Vehicle Control	Losartan	Prednisolone Acetate	Losartan + Prednisolone Acetate
Vehicle control	X	0.02	0.02	0.02
Losartan		X	0.19	0.88
Prednisolone acetate			X	0.08
Losartan + prednisolone acetate				X

**Table 3.** Kruskal–Wallis *P* Values Slit-Lamp Total Intensity Units

Characteristic	Vehicle Control	Losartan	Prednisolone Acetate	Losartan + Prednisolone Acetate
Vehicle control	X	0.02	0.08	0.02
Losartan		X	0.15	0.77
Prednisolone acetate			X	0.08
Losartan + prednisolone acetate				X

### IHC for Keratocan-Positive Keratocytes and $\alpha$ -SMA-Positive Myofibroblasts

Figure 2A shows representative central sections from corneas in each group. All corneas with alkali injury in this study had no corneal endothelium within the central 6 to 10 mm at 1 month after injury. No  $\alpha$ -SMA-positive myofibroblasts were found in any uninjured cornea. All corneas treated with BSS vehicle had full-thickness or nearly full-thickness  $\alpha$ -SMA-positive myofibroblasts, although some patches of keratocan-positive keratocytes were present, as shown in Figure 2A. In corneas treated with losartan alone,  $\alpha$ -SMA-positive myofibroblasts were confined mostly to the posterior half of the stroma in all corneas, as shown in the example in Figure 2A. The  $\alpha$ -SMA-positive myofibroblast localization tended to be more variable in the prednisolone acetate group. In two corneas in that group, the  $\alpha$ -SMA-positive myofibroblasts were found throughout the stroma (as shown in example 1 in Fig. 2A), and in two corneas, the  $\alpha$ -SMA-positive myofibroblasts were present only in the posterior half of the stroma (as shown in example 2 in Fig. 2A). In all four corneas in the losartan + prednisolone acetate combined group, the  $\alpha$ -SMA-positive myofibroblasts were confined to the far posterior stroma, with repopulation of the more anterior stroma with keratocan-positive keratocytes (as shown in Fig. 2A).

Supplementary Figure S2 shows  $\alpha$ -SMA-positive staining in a representative section from each cornea that was used for ImageJ analysis of the total area of stromal  $\alpha$ -SMA-positive staining and the total  $\alpha$ -SMA-positive opacity. The variability of stroma  $\alpha$ -SMA-positive staining in the prednisolone acetate

group can be noted in this figure. ImageJ analysis results for the total  $\alpha$ -SMA area in each cornea is shown in Figure 2B. Table 4 shows the statistical comparisons between the groups. The combined losartan-prednisolone acetate group had significantly less  $\alpha$ -SMA area than the vehicle control group. The combined losartan-prednisolone acetate group also had significantly less  $\alpha$ -SMA area than the prednisolone acetate group. Other differences did not reach statistical significance, although it can be noted there was a trend toward the losartan group being significantly different from the vehicle control group. ImageJ analysis results for the total  $\alpha$ -SMA opacity intensity in pixels for each cornea are shown in Figure 2C. Table 5 shows the statistical comparisons between the groups. Again, the combined losartan-prednisolone acetate group had highly significantly less  $\alpha$ -SMA opacity intensity in pixels than the vehicle control group. Also, the combined losartan-prednisolone acetate group was significantly less than the prednisolone acetate alone group in total  $\alpha$ -SMA opacity intensity. Other differences did not reach statistical significance. Importantly, note the low variability for both the total  $\alpha$ -SMA area (Fig. 2B) and the total  $\alpha$ -SMA opacity intensity (Fig. 2C) in the combined losartan + prednisolone acetate group.

### Immunohistochemical Analysis of Collagen Type IV Expression

Figure 3A shows representative duplex IHC for collagen type IV and TGF- $\beta$ 1 in the anterior and posterior stroma for representative corneas in each group and also shows example ImageJ quantitation rectangles. Figure 3B shows quantitation for collagen

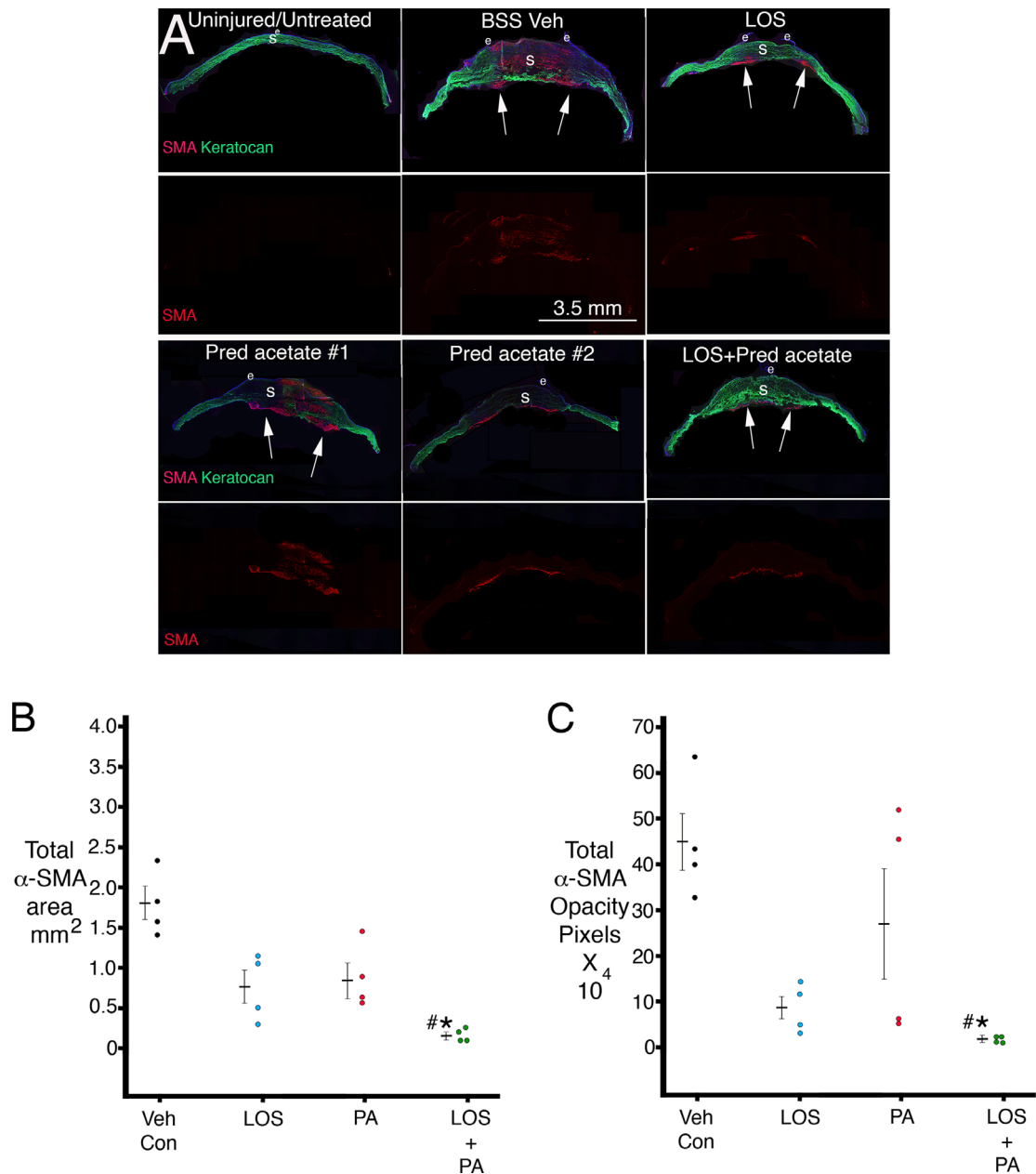


**Figure 2.** (A) Duplex immunohistochemistry for keratocyte-specific marker keratocan (green) and myofibroblast-specific marker  $\alpha$ -SMA (red) in uninjured control corneas and after alkali burn injury and 1 month of topical treatment. Fragile peripheral epithelium and persistent epithelial defects were noted in all alkali-burned corneas. In corneas treated with losartan alone or combination losartan + prednisolone acetate,  $\alpha$ -SMA-positive myfibroblasts tended to be localized to the posterior cornea, and the anterior cornea was repopulated by keratocan-positive keratocytes. Two examples of corneas treated with prednisolone acetate alone are shown to demonstrate the variability noted in this group. In #1,  $\alpha$ -SMA-positive myfibroblasts populated the entire thickness of this cornea, with a persistent epithelial defect. In #2,  $\alpha$ -SMA-positive myfibroblasts were present only in the posterior stroma despite the presence of a persistent epithelial defect. All alkali-burned corneas were devoid of corneal endothelium over an 8- to 10-mm diameter area of the posterior cornea. Arrows indicate areas with posterior  $\alpha$ -SMA-positive myfibroblasts. LOS is topical losartan. Pred acetate is 1% prednisolone acetate. BSS Veh is balanced salt solution vehicle. e is epithelium. S is stroma. (B) A graph of total  $\alpha$ -SMA-positive stromal area determined in central sections of each cornea in each group using ImageJ. \* indicates the mean was significantly different from the BSS vehicle control group. # indicates the mean was significantly different from the prednisolone acetate alone group. Table 4 shows Kruskal–Wallis *P* values for statistical comparisons between the groups. (C) A graph of total  $\alpha$ -SMA-positive intensity per corneal section in pixels determined in central sections of each cornea in each group using ImageJ. \* indicates the mean was significantly different from the BSS vehicle control group. # indicates the mean was significantly different from the prednisolone acetate-alone group. Note the lower mean and standard error of the mean in the combined losartan + prednisolone acetate group and the higher mean and standard error of the mean in the prednisolone acetate only group. Table 5 shows Kruskal–Wallis *P* values for statistical comparisons between the groups.

**Table 4.** Kruskal–Wallis *P* Values IHC SMA ImageJ Area

Characteristic	Vehicle Control	Losartan	Prednisolone Acetate	Losartan + Prednisolone Acetate
Vehicle control	X	0.06	0.14	0.0005
Losartan		X	0.71	0.10
Prednisolone acetate			X	0.04
Losartan + prednisolone acetate				X

**Table 5.** Kruskal–Wallis *P* Values IHC SMA Total Intensity Units

Characteristic	Vehicle Control	Losartan	Prednisolone Acetate	Losartan + Prednisolone Acetate
Vehicle control	X	0.10	0.55	0.002
Losartan		X	0.29	0.14
Prednisolone acetate			X	0.01
Losartan + prednisolone acetate				X

type IV staining intensity in the anterior stroma of the corneas in each group. Both losartan treatment and losartan + 1% prednisolone acetate significantly decreased the mean intensity units of collagen type IV in the anterior stroma compared to vehicle treatment. Prednisolone acetate alone produced a trend toward a decrease in collagen type IV staining intensity in the anterior stroma compared to vehicle treatment, but the difference did not reach statistical significance. Table 6 shows the statistical comparisons for collagen type IV intensity in the anterior stroma between the groups. Figure 3C shows quantitation for collagen type IV staining intensity in the posterior stroma of the corneas in each group. Only the topical losartan treatment was significantly different from the vehicle treatment, although the combined losartan + 1% prednisolone acetate group trended toward significance. Table 7 shows the statistical comparisons for collagen type IV intensity in the anterior posterior between the groups.

## Discussion

Chemical injuries to the cornea caused by NaOH vary from mild, self-limited ocular surface disturbances to devastating burns affecting the corneal epithelium, corneal limbus, stroma, and the corneal endothelium.<sup>23,25–30</sup> Severe alkali burn injuries are frequently associated with CNV and persistent epithelial defects.<sup>25–30</sup> Severe NaOH corneal burns can also injure the trabecular meshwork, iris, ciliary body, lens, retina, and optic nerve.<sup>25</sup>

The 1N NaOH corneal burn injury method used in the present study was used in many prior rabbit

studies.<sup>23,26,27</sup> The 1-month time point for analysis of the effect of alkali burn injury and the potential effects of the topical medications were selected because 1 month was when the wound-healing response to injury to the cornea peaked in prior studies.<sup>5,17–20</sup> The current study showed that severe chemical injury with 100  $\mu$ L 1N NaOH delivered using a 5-mm filter paper delivery system for 1 minute penetrated through the stroma and uniformly injured a large underlying area of the corneal endothelium, and often Descemet's membrane, approximately 8 to 10 mm in diameter. No evidence of limbal injury was noted using this method. Similarly, no evidence of iris or lens damage was noted in the rabbit eyes after this injury. In preliminary experiments, even 15 seconds of exposure to 1N NaOH using this method damaged the corneal endothelium (L.P. Sampaio and S.E. Wilson, unpublished data, 2021), and, therefore, dilutions of the NaOH would likely be needed to produce a model with injury confined to the epithelium and anterior stroma of the cornea.

The mode of cell death of the affected epithelium, keratocytes, and corneal endothelium produced by the 1N NaOH was previously reported to be necrosis.<sup>28,29</sup> Cellular necrosis, along with denaturation of the underlying collagen fibrils,<sup>30</sup> likely triggered the severe corneal inflammatory response that was noted with the slit lamp in all corneas in this study during the first few days to 2 weeks after injury.

The opacities remaining at 1 month after injury and treatment in all groups were characterized by a dense central zone surrounded by a less dense ring (Fig. 1A). We hypothesize that the dense central area represents denatured and disorganized collagen fibrils produced



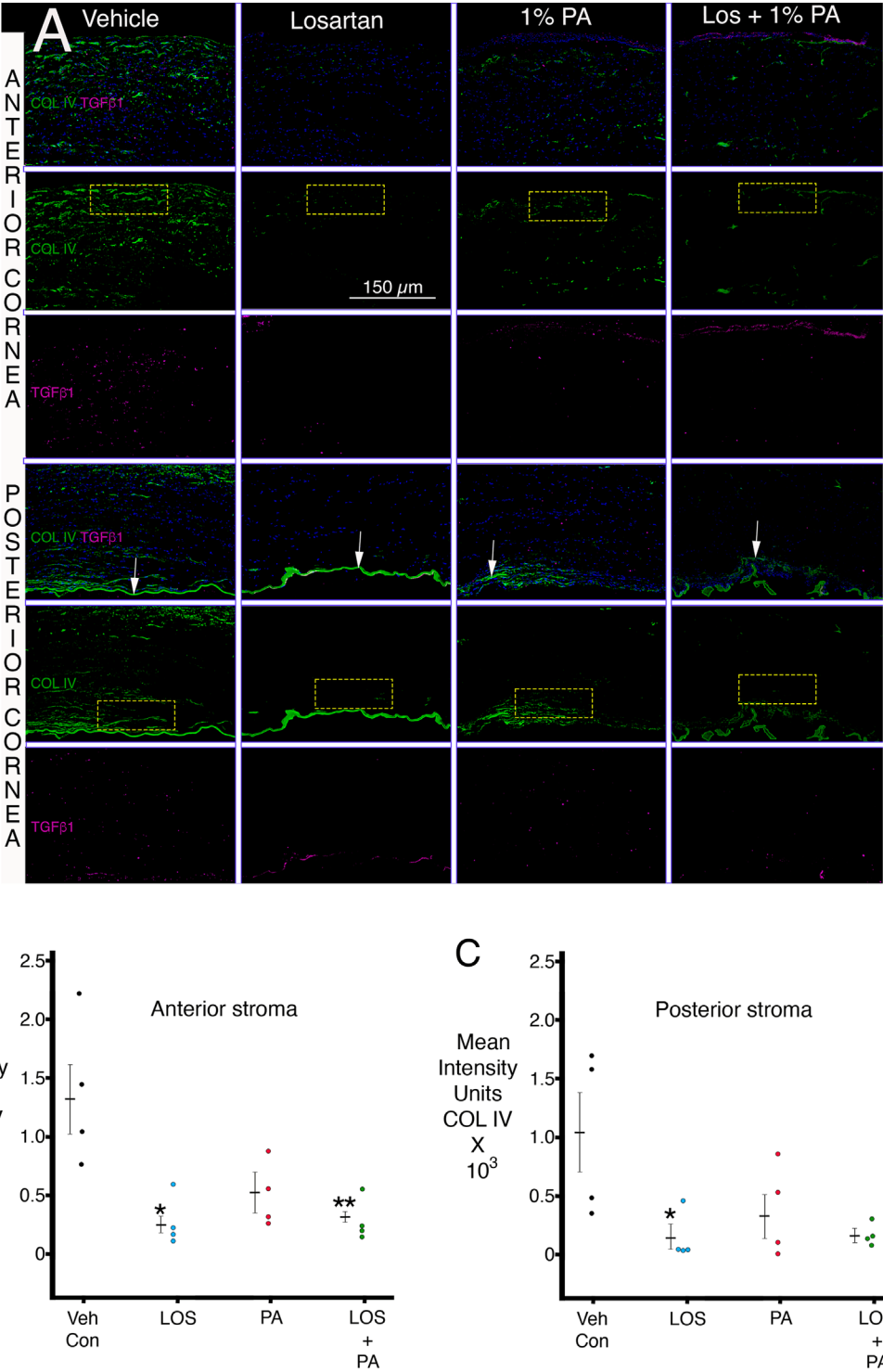


**Figure 3.** Duplex immunohistochemistry for TGF-β1 and collagen type IV in both the anterior stroma and posterior stroma. **(A)** Representative IHCs for each group are shown. *Arrows* indicate Descemet’s membrane or remnants of Descemet’s membrane in each cornea. Representative ImageJ quantitation rectangles (100 × 50 units) for both the anterior stroma (long side of *rectangle* at anterior stromal surface) and the posterior stroma (long side of *rectangle* at posterior stromal surface just anterior to Descemet’s membrane or its remnants). No differences in TGF-β1 were noted between the groups. **(B)** ImageJ quantitation of collagen type IV IHC intensity units in the anterior stroma in the groups. \* and \*\* indicate the mean was significantly different from the vehicle group. [Table 6](#) shows Kruskal–Wallis *P* values for statistical comparisons between the groups. **(C)** ImageJ quantitation of collagen type IV IHC intensity units in the posterior stroma in the groups. \* indicates the mean was significantly different from the vehicle group. [Table 6](#) shows Kruskal–Wallis *P* values for statistical comparisons between the groups.

**Table 6.** Kruskal–Wallis *P* Values Anterior Stromal Mean Intensity Units

Characteristic	Vehicle Control	Losartan	Prednisolone Acetate	Losartan + Prednisolone Acetate
Vehicle control	X	0.004	0.16	0.01
Losartan		X	0.14	0.71
Prednisolone acetate			X	0.27
Losartan + prednisolone acetate				X

**Table 7.** Kruskal–Wallis *P* Values Posterior Stromal Mean Intensity Units

Characteristic	Vehicle Control	Losartan	Prednisolone Acetate	Losartan + Prednisolone Acetate
Vehicle control	X	0.01	0.15	0.07
Losartan		X	0.30	0.50
Prednisolone acetate			X	0.71
Losartan + prednisolone acetate				X

by the original NaOH injury, along with myofibroblasts that developed and the large amounts of disordered extracellular matrix these fibrotic cells produced.<sup>5,20,31</sup> The less dense ring may be associated with less severely damaged stromal collagen and corneal fibroblasts, along with lesser amounts of disordered extracellular matrix produced by corneal fibroblasts, although further investigation would be needed to confirm this hypothesis.

In a prior study,<sup>7</sup> topical 0.4 mg/mL losartan six times per day decreased corneal scarring and stromal myofibroblasts after descemetorhexis injury to the corneal endothelium and Descemet's membrane. In the present study, topical treatment with 0.2 mg/mL losartan in BSS, 1% prednisolone acetate, or combined losartan and prednisolone acetate six times per day decreased the total corneal opacity area measured with ImageJ on the standardized slit-lamp images (Fig. 1B). The differences in the total area of opacity were not significantly different between the losartan, prednisolone acetate, or combined losartan/prednisolone acetate groups (Table 2). The total opacity in pixels in the opacified area of cornea, also measured with ImageJ, was significantly lower in the 0.2-mg/mL losartan group or the combined 0.2-mg/mL losartan + 1% prednisolone acetate group compared to the vehicle BSS group. The 1% prednisolone acetate alone group trended toward decreased total opacity compared to the vehicle BSS group, but the difference did not reach statistical significance (Table 3).

The most interesting findings in this study relate to myofibroblast development and stromal fibrosis in the different treatment groups (Fig. 2A). All corneas that had the alkali burn followed by treat-

ment with vehicle BSS had  $\alpha$ -SMA-positive myofibroblasts and fibrosis throughout the full thickness of the cornea, although this fibrosis appeared to be greatest adjacent to the anterior and posterior stromal surfaces (Supplementary Fig. S2), likely due to higher concentrations of TGF- $\beta$ 1 and TGF- $\beta$ 2 penetrating the stroma from the tears, epithelium, residual peripheral corneal endothelium, and aqueous humor at the corneal surfaces.<sup>5,20</sup> In the NaOH-injured corneas treated with topical 0.2 mg/mL losartan, the greatest density of  $\alpha$ -SMA-positive myofibroblasts tended to be noted in the posterior half of the stroma, although lesser amounts of anterior stromal  $\alpha$ -SMA-positive myofibroblasts were noted in the two losartan-treated corneas after 1 month of treatment (Supplementary Fig. S2). Persistent corneal epithelial defects are themselves associated with the development of anterior stromal myofibroblasts and fibrosis<sup>32</sup> and could have had a role in anterior myofibroblasts noted in two losartan-treated corneas. Alkali-injured corneas treated with 1% prednisolone acetate alone were more variable in stromal myofibroblast development (Supplementary Fig. S2). After injury and treatment with combined losartan and prednisolone acetate, however, the  $\alpha$ -SMA-positive myofibroblasts in all four corneas were restricted to the far posterior stroma (Supplementary Fig. S2). It is important to note that the corneal endothelium and Descemet's membrane had not regenerated in any cornea in any of the treatment groups by the 1-month time point, as can be noted in the representative corneas in Figure 2A.

When the area of  $\alpha$ -SMA-positive myofibroblasts was determined using ImageJ in each of the

central corneas (Fig. 2B), the combined losartan + prednisolone acetate group was significantly different from the vehicle BSS-treated group ( $P = 0.0005$ , Table 4). This combined losartan + prednisolone acetate group also had low standard error of the mean for the area of  $\alpha$ -SMA staining (Fig. 2B). The combined losartan and prednisolone acetate group had a significantly lower area of  $\alpha$ -SMA staining than the prednisolone acetate-alone group. Similarly, when the total  $\alpha$ -SMA intensity per corneal section was determined using ImageJ in each of the corneas (Fig. 2C), the combined losartan + prednisolone acetate treatment group was significantly lower than the vehicle BSS-treated group ( $P = 0.002$ , Table 5), and the combined losartan + prednisolone acetate treatment group was significantly lower than the prednisolone acetate-alone group ( $P = 0.01$ ). We hypothesize that the efficacy of the combined losartan + prednisolone acetate treatment after the severe alkali burns was attributable to the corticosteroid modulation of inflammation due to the severe tissue necrosis and the losartan modulation of profibrotic TGF- $\beta$  effects on stromal myofibroblast development and, therefore, disordered collagen production by these cells. Bone marrow-derived fibrocytes also enter the stroma from the limbus after injury and, in addition to corneal fibroblasts, are TGF- $\beta$ -driven precursors to myofibroblasts.<sup>33,34</sup> Corticosteroids inhibit the proliferation of fibrocytes necessary for generation of large numbers of myofibroblasts<sup>35</sup> and also trigger fibrocyte apoptosis.<sup>36</sup> Thus, the topical corticosteroids could contribute to losartan inhibition of myofibroblast development from both corneal fibroblasts and fibrocytes via these mechanisms.

One limitation of this study was that treatments after alkali burn injury were only applied for 1 month after injury. However, a decrease in myofibroblasts in the stroma is a first step to the resolution of fibrosis,<sup>5,20</sup> since it allows for the migration of corneal fibroblasts, and eventually keratocytes, from the peripheral cornea into the injured tissue. These stromal cells function to reabsorb damaged collagens and other matrix materials and regenerate ordered stromal collagen fibrils associated with corneal transparency.<sup>5,19–22</sup> We hypothesize that longer treatment with topical losartan and prednisolone acetate, probably for at least several months to a year, would produce a further increase in corneal transparency since stromal myofibroblast area and intensity of  $\alpha$ -SMA staining were markedly and consistently decreased when both medications were applied (Figs. 2B, 2C). Once the myofibroblasts are eliminated, keratocytes and corneal fibroblasts can begin the slow process of removing and reorganizing the disordered extracellular matrix

that contributes to the scarring and eventually may restore transparency. Whether or not this leads to sufficient vision to reduce the need for corneal transplantation requires further study. Certainly, other factors, such as insufficient inhibition of TGF- $\beta$  signaling by losartan and/or the effects of other growth factors, such as PDGF, could influence this efficacy of losartan on long-standing scars. Further studies in animals and humans will be needed to determine the efficacy of the losartan and topical corticosteroid combination in established corneal scars. Another explanation for why a greater increase in transparency was not noted after 1 month of losartan-prednisolone acetate treatment is that the corneal endothelium was not yet regenerated. Even after a simple 8-mm descemetorhexis in rabbits, the corneal endothelium and Descemet's membrane do not regenerate until 4 to 6 months after the injury.<sup>37</sup> Thus, some of the opacity is due to stromal edema. Full recovery of transparency, especially in human corneas with lower corneal endothelial proliferative potential, may require simultaneous treatment with rho-kinase inhibitors to stimulate corneal endothelial proliferation<sup>38</sup> or endothelial replacement surgery.

All alkali-burned corneas in this study treated with BSS vehicle six times a day developed moderate to severe CNV that further compromises corneal transparency and vision (Fig. 1A, Supplementary Fig. S1). Further study is needed to determine if losartan plus corticosteroid therapy alone could provide effective treatment to reduce CNV after severe corneal injuries or whether the application of other inhibitors of CNV would be needed.

This study demonstrated that severe sodium hydroxide injuries are commonly associated with damage to the corneal endothelium and Descemet's membrane that increase the corneal fibrosis response. This is analogous to findings regarding the effects of chemical burns caused by bioweapon agents, such as sulfur mustard, where corneal endothelial damage was a major determinate of the long-term outcomes of injury.<sup>39,40</sup> Combined topical losartan and corticosteroids could also decrease myofibroblast generation and corneal scarring fibrosis that occur in response to these chemical bio-weapon agents.

This study also found that collagen type IV produced by corneal fibroblasts, which was not associated with the epithelial BM or Descemet's BM, was upregulated in the stroma after alkali burn injury, similar to what was noted after descemetorhexis injury in prior studies.<sup>7,22</sup> The increase was most prominent in the anterior and posterior stroma, nearest to the tear film and aqueous humor sources of TGF- $\beta$ 1 and TGF- $\beta$ 2.<sup>5,22</sup> TGF- $\beta$ 1 directly stimulates corneal

fibroblasts to upregulate collagen type IV production.<sup>7</sup> Since collagen type IV directly binds TGF- $\beta$ 1 and TGF- $\beta$ 2<sup>41,42</sup> and prevents their binding to the cognate TGF- $\beta$  receptors, thereby modulating the effects of TGF- $\beta$  on stromal cells, this collagen type IV upregulation likely represents a feedback regulatory pathway to modulate the effects of TGF- $\beta$  on corneal fibroblasts, myofibroblasts, and other stromal cells.<sup>7</sup> This regulatory pathway is also likely active in other organs where injuries trigger fibrosis and organ dysfunction.<sup>43</sup> Losartan, via its modulation of TGF- $\beta$  signaling, decreased collagen type IV production in the stroma after alkali burn injury, similar to what was found in the descemetorhexis injury model in rabbits.<sup>7</sup> This decrease in collagen type IV production extending to the posterior stroma confirms topical losartan penetration into the stroma.

In conclusion, combined topical treatment with losartan and corticosteroids most effectively decreased corneal opacity and stromal myofibroblast generation after severe alkali burn injury. Further study is needed to optimize the dosing regimens and the timing of treatment after injury to provide effective therapy for chemical burns in humans.

## Acknowledgments

The authors thank Winston Kao, PhD, for providing the keratocan antibody utilized in this study and Ajaykumar Zalavadia of the Imaging Core lab at Lerner Research Institute of the Cleveland Clinic with assistance photographing sections. Supported in part by Department of Defense grant VR180066 (SEW) and P30-EY025585 from the National Eye Institute, National Institutes of Health (Bethesda, MD, USA) and Research to Prevent Blindness (New York, NY, USA).

Disclosure: **L.P. Sampaio**, None; **G.S.L. Hilgert**, None; **T.M. Shiju**, None; **M.R. Santhiago**, None; **S.E. Wilson**, submitted a provisional patent to the US Patent Office regarding topical use of losartan and other angiotensin converting enzyme II receptor inhibitors to decrease corneal scarring fibrosis after injury (P)

## References

1. Witcher J, Srinivasan M, Upadhyay MP. Corneal blindness: a global perspective. *Bull World Health Organ*. 2001;79:214–221.
2. Wilson SE. Corneal wound healing. *Exp Eye Res*. 2020;197:109089.
3. Ljubimov AV, Saghizadeh M. Progress in corneal wound healing. *Prog Retin Eye Res*. 2015;49:17–45.
4. Jester JV, Huang J, Petroll WM, Cavanagh HD. TGFbeta induced myofibroblast differentiation of rabbit keratocytes requires synergistic TGF-beta, PDGF and integrin signaling. *Exp Eye Res*. 2002;75:645–657.
5. de Oliveira RC, Tye G, Sampaio LP, et al. TGF $\beta$ 1 and TGF $\beta$ 2 proteins in corneas with and without stromal fibrosis: delayed regeneration of epithelial barrier function and the epithelial basement membrane in corneas with stromal fibrosis. *Exp Eye Res*. 2021;202:108325.
6. Wilson SE. TGF beta -1, -2 and -3 in the modulation of fibrosis in the cornea and other organs. *Exp Eye Res*. 2021;207:108594.
7. Sampaio LP, Hilgert GSL, Shiju TM, Murillo SE, Santhiago MR, Wilson SE. Topical losartan inhibits corneal scarring fibrosis and collagen type IV deposition after Descemet's membrane-endothelial excision in rabbits. *Exp Eye Res*. 2022;216:108940.
8. Wylie-Sears J, Levine R, Bischoff J. Losartan inhibits endothelial-to-mesenchymal transformation in mitral valve endothelial cells by blocking transforming growth factor- $\beta$ -induced phosphorylation of ERK. *Biochem Biophys Res Commun*. 2014;446:870–875.
9. Geirsson A, Singh M, Ali R, et al. Modulation of transforming growth factor- $\beta$  signaling and extracellular matrix production in myxomatous mitral valves by angiotensin II receptor blockers. *Circulation*. 2012;126(11, suppl 1):S189–S197.
10. Park JK, Ki MR, Lee EM, et al. Losartan improves adipose tissue-derived stem cell niche by inhibiting transforming growth factor- $\beta$  and fibrosis in skeletal muscle injury. *Cell Transplant*. 2012;21:2407–2424.
11. Lim D-S, Lutucuta S, Bachireddy P, et al. Angiotensin II blockade reverses myocardial fibrosis in a transgenic mouse model of human hypertrophic cardiomyopathy. *Circulation*. 2001;103:789–791.
12. Lavoie P, Robitaille G, Agharazii M, et al. Neutralization of transforming growth factor-beta attenuates hypertension and prevents renal injury in uremic rats. *J Hypertens*. 2005;23:1895–1903.
13. Cohn RD, Erp C, Van Habashi JP, et al. Angiotensin II type 1 receptor blockade attenuates TGF- $\beta$ -induced failure of muscle regeneration in multiple myopathic states. *Nat Med*. 2007;13:204–210.



14. Wu M, Peng Z, Zu C, Ma J, Lu S, Zhong J, Zhang S. Losartan attenuates myocardial endothelial-to-mesenchymal transition in spontaneous hypertensive rats via inhibiting TGF- $\beta$ /Smad signaling. *PLoS One*. 2016;11:e0155730.
15. Yao Q, Qian JQ, Lin XH, Lindholm B. Inhibition of the effect of high glucose on the expression of Smad in human peritoneal mesothelial cells. *Int J Artif Organs*. 2004;27:828–834.
16. Wylie-Sears J, Levine RA, Bischoff J. Losartan inhibits endothelial-to-mesenchymal transformation in mitral valve endothelial cells by blocking transforming growth factor- $\beta$ -induced phosphorylation of ERK. *Biochem Biophys Res Commun*. 2014;446:870–875.
17. Torricelli AAM, Singh V, Agrawal V, Santhiago MR, Wilson SE. Transmission electron microscopy analysis of epithelial basement membrane repair in rabbit corneas with haze. *Invest Ophthalmol Vis Sci*. 2013;54:4026–4033.
18. Marino GK, Santhiago MR, Santhanam A, et al. Regeneration of defective epithelial basement membrane and restoration of corneal transparency. *J Ref Surg*. 2017;33:337–346.
19. Marino GK, Santhiago MR, Santhanam A, et al. Epithelial basement membrane injury and regeneration modulates corneal fibrosis after pseudomonas corneal ulcers in rabbits. *Exp Eye Res*. 2017;161:101–105.
20. de Oliveira RC, Sampaio LP, Shiju TM, Santhiago MR, Wilson SE. Epithelial basement membrane regeneration after PRK-induced epithelial-stromal injury in rabbits: fibrotic vs. non-fibrotic corneal healing. *J Ref Surg*. 2022;38:50–60.
21. Medeiros CS, Marino GK, Santhiago MR, Wilson SE. The corneal basement membranes and stromal fibrosis. *Invest Ophthalmol Vis Sci*. 2018;59:4044–4053.
22. Sampaio LP, Shiju TM, Hilgert GSL, et al. Descemet's membrane injury and regeneration, and posterior corneal fibrosis in rabbits. *Exp Eye Res*. 2021;213:108803.
23. Ishizaki M, Zhu G, Haseba T, Shafer SS, Kao WW. Expression of collagen I, smooth muscle alpha-actin, and vimentin during the healing of alkali-burned and lacerated corneas. *Invest Ophthalmol Vis Sci*. 1993;34:3320–3328.
24. Nirankari VS, Dandona L, Rodrigues MM. Laser photocoagulation of experimental corneal stromal vascularization: efficacy and histopathology. *Ophthalmology*. 1993;100:111–118.
25. Paschalis EI, Zhou C, Lei F, et al. Mechanisms of retinal damage after ocular alkali burns. *J Pathol*. 2017;187:1327–1342.
26. Lee HS, Lee JH, Kim CE, Yang JW. Anti-neovascular effect of chondrocyte-derived extracellular matrix on corneal alkaline burns in rabbits. *Graefes Arch Clin Exp Ophthalmol*. 2014;252:951–961.
27. Burns FR, Stack MS, Gray RD, Paterson CA. Inhibition of purified collagenase from alkali-burned rabbit corneas. *Invest Ophthalmol Vis Sci*. 1989;30:1569–1575.
28. Yi K, Chung TY, Hyon JY, Koh JW, Wee WR, Shin YJ. Combined treatment with antioxidants and immunosuppressants on cytokine release by human peripheral blood mononuclear cells—chemically injured keratocyte reaction. *Mol Vis*. 2011;17:2665–2671.
29. Renard G, Hirsch M, Pouliquen Y. Corneal changes due to alkali burns. *Trans Ophthalmol Soc UK*. 1978;98:379–382.
30. Maskati QB, Maskati BT. Management of chemical injuries of the eye. *Ind J Ophthalmol*. 1987;35:396–400.
31. Jester JV, Moller-Pedersen T, Huang J, et al. The cellular basis of corneal transparency: evidence for 'corneal crystallins'. *J Cell Sci*. 1999;112:613–622.
32. Wilson SE, Medeiros CS, Santhiago MR. Pathophysiology of corneal scarring in persistent epithelial defects after PRK and other corneal injuries. *J Ref Surg*. 2018;34:59–64.
33. Lassance L, Marino GK, Medeiros CS, Thangavadiel S, Wilson SE. Fibrocyte migration, differentiation and apoptosis during the corneal wound healing response to injury. *Exp Eye Res*. 2018;170:177–187.
34. de Oliveira RC, Wilson SE. Fibrocytes, wound healing and corneal fibrosis. *Invest Ophthalmol Vis Sci*. 2020;61:28–35.
35. Hayashi H, Kawakita A, Okazaki S, Murai H, Yasutomi M, Ohshima Y. IL-33 enhanced the proliferation and constitutive production of IL-13 and IL-5 by fibrocytes. *Biomed Res Int*. 2014;2014:738625.
36. Lo CY, Michaeloudes C, Bhavsar PK, et al. Increased phenotypic differentiation and reduced corticosteroid sensitivity of fibrocytes in severe asthma. *J Allergy Clin Immunol*. 2015;135:1186–1195.e1–6.
37. Sampaio LP, Shiju TM, Hilgert GSL, et al. Descemet's membrane injury and regeneration, and posterior corneal fibrosis in rabbits. *Exp Eye Res*. 2021;213:108803.
38. Okumura N, Sakamoto Y, Fujii K, et al. Rho kinase inhibitor enables cell-based therapy for corneal endothelial dysfunction. *Sci Rep*. 2016;6:26113.

39. McNutt P, Tuznik K, Nelson M, et al. Structural, morphological, and functional correlates of corneal endothelial toxicity following corneal exposure to sulfur mustard vapor. *Invest Ophthalmol Vis Sci.* 2013;54:6735–6744.
40. McNutt PM, Nguyen DL, Nelson MR, et al. Corneal endothelial cell toxicity determines long-term outcome after ocular exposure to sulfur mustard vapor. *Cornea.* 2020;39:640–648.
41. Paralkar VM, Vukicevic S, Reddi AH. Transforming growth factor beta type 1 binds to collagen IV of basement membrane matrix: implications for development. *Dev Biol.* 1991;143:303–308.
42. Shibuya H, Okamoto O, Fujiwara S. The bioactivity of transforming growth factor-beta 1 can be regulated via binding to dermal collagens in mink lung epithelial cells. *J Dermatol Sci.* 2006;41:187–195.
43. Wilson SE, Shiju TM, Sampaio LP, Hilgert GSL. Corneal fibroblast collagen type IV negative feedback modulation of TGF beta: a fibrosis modulating system likely active in other organs. *Matrix Bio.* 2022;109:162–172.